DOI 10.5162/sensor2017/D2.3

An All-Inkjet Printed Sensor System Embedded in Injection-Moulded Plastics

Christoph Beisteiner[1], Thomas Mitterlehner[2], Thomas Thurner[1] and Bernhard Zagar[1]
Johannes Kepler University Linz, Altenbergerstr. 69, 4040 Linz, Austria
[1]Institute for Measurement Technology
[2]Institute of Polymer Injection Moulding and Process Automation
christoph.beisteiner@jku.at, bernhard.zagar@jku.at

Abstract:
Inkjet-printing enables the fabrication of low-cost sensor systems without the need of a photo mask and can be used for rapid prototyping. By using a commercially available Epson inkjet printer and silver nanoparticle dispersion, electrically conductive traces can be easily printed on photo paper or other substrates of interest. In order to protect the printed circuits from environmental influences, the sensor circuits can be embedded into plastic. In this paper a fully inkjet-printed sensor system consisting of a thermocouple and a strain gauge was developed as a functional model and finally protected from environmental conditions by an injection-molding process. In this context the Seebeck-coefficient of various inkjet-printable materials as well as the gauge factor of the used substrate were characterized.

Key words: injection-molding, seebeck-coefficient, gauge factor

Introduction

Functional materials can be printed by using inkjet or screen printing technology to develop flexible or wearable displays and sensor systems. Low-cost Piezo-Jet (e.g. Epson, Brother, Ricoh) or Bubble-Jet (e.g. Canon, HP, Lexmark, Olivetti) based printers with silver nanoparticle-based (NAg) dispersions from Mitsubishi can be used to directly print electrically conductive traces. Strain gauges, resistive temperature devices (RTDs) or capacitive sensors can easily be manufactured on resin-coated paper or coated PET film substrates like Mitsubishi, HP, Epson or Canon [1]. Furthermore, thermocouples have already been printed using conductive polymers with thick-film technology for temperature measurements [2], [3]. Finally, surface-mounted devices (SMD) can be soldered directly onto the printed traces. Nevertheless, the bonding strength between the paper and the soldered components is not comparable to conventional PCBs.

Above all the printed silver nanolayers are sensitive to mechanical wear and change their electrical conductivity over time due to oxidation. By overprinting the layers with an electrically non-conductive polymer e.g. Polyvinylalcohol (PVA), the scratching resistance can be improved and the oxidation process can be reduced [4].

Another approach to protect the printed nanolayers and the soldered components from oxidation is by embedding the printed substrates into plastic components.

In this paper we report an inkjet-printed sensor system consisting of a strain gauge and a thermocouple that was developed and finally embedded into polyethylene (PE) by using an injection molding process.

Inkjet-printed structures

Conductive polymers or nanoparticle-based dispersions can be inkjet-printed by using the drop-on-demand (DOD) technology. The most commonly used DOD technologies are bubble-jet or piezoelectric-jet based. The former process involves ejecting the ink from a chamber by causing a rapid vaporization by heating the ink, the latter process involves generating a pressure pulse in the fluid which forces an ink droplet from the nozzle [5].

In this work a six-color Epson Stylus Photo 1500W low-cost printer with a Micro Piezo print head is used, since it shows flexibility to a wide range of ink viscosities $1\,\mathrm{mPa\,s}$ to $15\,\mathrm{mPa\,s}$ and surface tensions $30\,\mathrm{mN\,m^{-1}}$ to $75\,\mathrm{mN\,m^{-1}}$ [4], [6]. Additionally a piezoelectric-jet based printer will not change the ink's properties, due to a heating process as it can be done by bubble-jet inkjet heads.

The genuine ink cartridges of the Epson printer are replaced with empty refill-cartridges, which are filled with micro filtered ($<$ 1.2 µm) water-based dispersions. The genuine ink of Epson has an average viscosity of 2.24 mPa s and a surface tension of 30.5 mN m^{-1} at 20°. The viscosity was measured with a vibro viscometer (AND SV-A [7]), while the surface tension was measured with a bubble pressure tensiometer (SITA DynoTester [8]).

Materials for Strain Gauges

Conductive structures were printed using a silver-nanoparticle ink NBSIJ-MU01 (NAg) from Mitsubishi with a viscosity of 2.9 mPa s and a surface tension of 32 mN m^{-1} at 20°, which is in the approximate range of the genuine ink.
A Pelikan Inkjet Overhead Transparency (PIOT) film with a surface energy of 57.5 mN m^{-1} was used as substrate, because it shows a good adhesion to PE, although the NAg layers on PIOT films can easily be removed by just touching them. The surface energy was estimated by measuring the contact angle of liquid droplets with known polar and dispersive components (water, n-Hexan and Ethylenglycol) on a PIOT film and using the OWRK method [9]. After printing on a PIOT film the electrical sheet resistance R_B of a silver nano layer can be decreased to $R_B =$ 0.09 Ω by a thermal sintering process at 80 °C for an annealing time of 20 min. This coalescence process changes the sizes and shapes of the silver nanoparticles and already takes place at temperatures far below the melting point of the bulk material. The final electrical conductivity has a value of $\sigma_{\text{Ag,sintered}} \approx 14 \times 10^6$ S m^{-1} at a typical layer thickness of 800 nm.
The sheet resistance was calculated by printing a meander structure and measuring its resistance R_L

$$R_L = R_B \cdot \frac{l}{b} \qquad (1)$$

with its length l and width b.

If a piezoresistive effect is assumed, the relation between a relative change in resistance and mechanical strain ϵ can be calculated by

$$K = \frac{\frac{\Delta R}{R_0}}{\epsilon}. \qquad (2)$$

A test structure (Fig. 1) with $R_0 =$ 77 Ω was printed on a PIOT film to characterize the strain gauge factor. The left and right ends of the structure are thicker to reduce the sensitivity along the transverse axis.

A tensile testing machine was used to measure the relative resistance change under stress. The inital force along the sensitive axis was set at 60 N. Different stress cycles were performed up to 130 N with a force step of 10 N.
The relative change in resistance of a small strain gauge 21.9 mm × 8.7 mm in sensitive and transverse axis of this substrate is shown in Fig. 2.

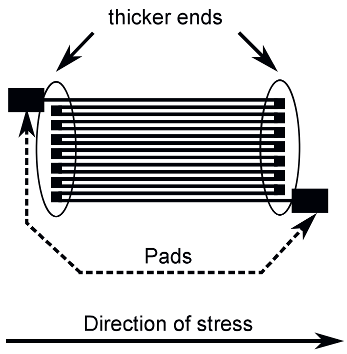

Fig. 1. Printed strain gauge to characterize the sensitivity in stress- and in transverse stress direction.

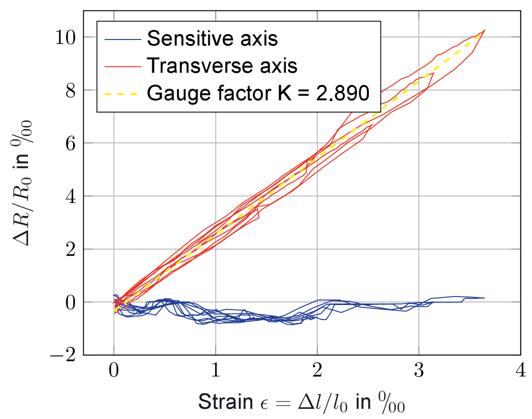

Fig. 2. Relative change in resistance of a printed strain gauge on a PIOT film in sensitive- and in transverse axis.

The sensitive axis shows a linear relation between $\frac{\Delta R}{R_0}$ and ϵ and one can observe only a small change in the transverse axis. The gauge factor along the sensitive axis results in $K = 2.890$. This is close to the gauge factor of bulk silver ($K = 3.004$), but it also depends on the used substrate and could thus be higher by even an order of magnitude, e.g. $K = 15.6$ on a Mitsubishi Nano Benefit Series or $K = 1.7$ on a HP Advanced Photo Paper [10]. A larger gauge factor can be caused by more pores in the substrate, that lead to more cracks and changes the connectivity between the silver nanoparticles [11].

Materials for Thermocouples

Thermocouples require at least two thermoelectrically different materials for generating a thermoelectric voltage. For low temperature differences ΔT over a conductor the thermoelectric voltage is given by

$$U_{th} = \overline{S}\Delta T \quad (3)$$

where $\overline{S}$ is the Seebeck coefficient.

In order to maximize the Seebeck coefficient different metallic nanoparticle based dispersions were prepared and printed on a test substrate. Also organic conducting materials can be used, such as Polyaniline (PANI), Polyacetylene (PA) or Poly-3,4-ethylendioxythiophen (PEDOT:PSS) [12].
A summary of the tested inks is given in Tab. 1.

Materials relative to NAg	$\overline{S}$ in µV K^{-1}	R_B in Ω/□
Carbon black	−1.95	10 k
Carbon nanotubes	−2.70	1.4 k
Ni	11.50	14.8 k
TiC	6.60	1.95 k
PEDOT:PSS (4 layers)	−23.25	1.16 k
ATO	40.00	110 k
ITO	27.50	100 k

Tab. 1: Parameters of tested inkjet-printable conductive materials. Favourable are materials with a low sheet resistance and high Seebeck coefficient.

A carbon nanotube ink is based on multi-walled carbon nanotubes, Pluronic F-127 and water and finally prepared as described in [13].
The carbon black ink was prepared with polyvinylpyrrolidone (PVP), Ketjenblack EC-600J and water. Finally a stable solution was achieved by final sonication and centrifugation process.
Commercial PEDOT:PSS (Clevios P Jet 700 N) was purchased from Heraeus as ready-to-use dispersion and diluted with water to reduce the viscosity of the final ink to 14 mPa s [14].
Antimon-Tin-Oxide (ATO) und Indium-Tin-Oxide (ITO) were purchased as dispersion from US Research Nanomaterials, Inc [15].
Nickel (Ni) and Titanium carbide (TiC) nanoparticles were purchased from US Research Nanomaterials, Inc. A dispersion based on Ni-nanoparticles, Polyvinylalkohol (PVA) and a surfactant (Disperbyk-111) was prepared, unfortunately the dispersion tends to cluster after a few days. A further dispersion with TiC-nanoparticles, PVA, and Disperbyk-111 was prepared. This dispersion also shows clusters after a few days.
Each ink was filtered with a 1.2 µm syringe filter and its surface tension and viscosity was adjusted to genuine ink's properties.

For estimating $\overline{S}$ prototype devices consisting of 5 thermocouples were prepared on a PIOT film. The thermoelectric device was directly connected with spring probes and heated in a hot chamber and cooled in a cold chamber while U_{th} and ΔT were measured. The temperature distribution in the hot as well as the cold chamber was kept homogeneous by fans (Fig. 3).

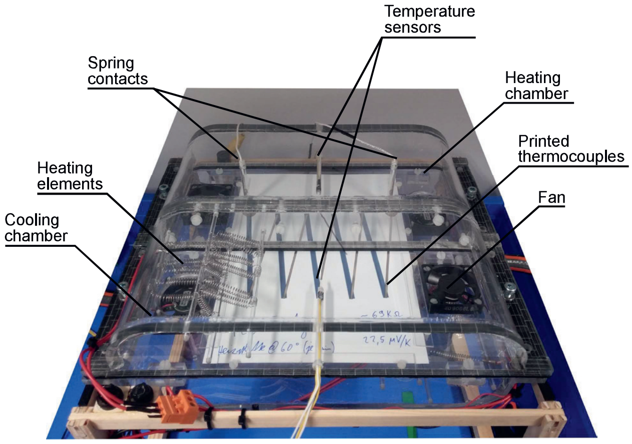

Fig. 3. Experimental setup to characterize the Seebeck coeffcient.

The best result was achieved with a PEDOT:PSS / NAg thermocouple 1, because this combination provides good tradeoff between a high Seebeck coefficient and a low sheet resistance. The PEDOT:PSS ink was printed with a viscosity of 13.6 mPa s and a surface tension of 35 mN m^{-2}. Although the viscosity of PEDOT:PSS is higher than the genuine ink, the solution was stable and results were reliably obtained. The Seebeck coefficient of PEDOT:PSS / NAg was also measured for some other substrates. The results show no impact of different substrates on the Seebeck coefficient.

Reducing the Sheet Resistance of PEDOT:PSS

A post-treatment process by thermally annealing the printed PEDOT:PSS layers to reduce the sheet resistance was performed. The resistance of a PEDOT:PSS structure (3 layers) was measured as a function of temperature while it was thermally annealed and is shown in Fig. 4.

The resistance dramatically reduces as solvents evaporate within the first 300 s, an even higher annealing temperature further reduces the resistance, because it leads to an increase in the chain movement and enhances the packing.

The sheet resistance of PEDOT:PSS can be further reduced by adding a suitable solvent, such as dimethylsulfoxid (DMSO) or ethylene glycol

(EG). These high boiling point solvents are well-known to increase the electrical conductivity [16]. Furthermore a suitable concentration of sorbitol (SB) also increases the electrical conductivity of PEDOT:PSS [17].

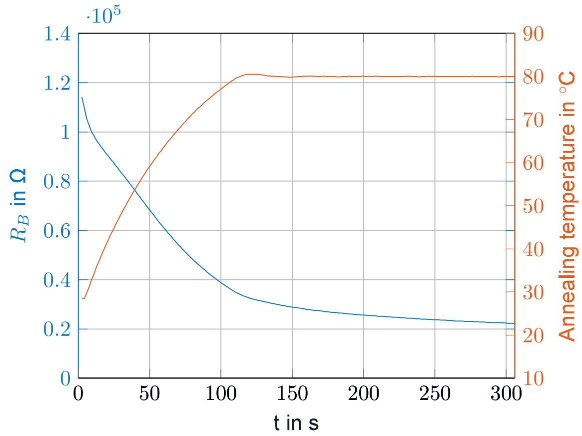

Fig. 4. Influence of the thermal annealing process of PEDOT:PSS to the sheet resistance immediately after printing.

A printer was used for mixing different components in order to find an optimal composition in terms of resistivity. PEDOT:PSS, DMSO, EG and sorbitol were prepared as independent inks and filled into Black, Cyan, Magenta and Yellow cartridges. Stripes of DMSO were printed with different color contrast levels (0% – 100%) and mixed with a contrast level of 50% Black (PEDOT:PSS). The resistivity of the stripes was measured. The lowest one represents the best mixture of the two components. Unfortunately, the contrast level is not equal to the ratio of components, due to the different properties of the inks. Therefore, the air intake of the ink cartridge was measured during a printing process and used to calculate the ratio of components.

An optimum was found at 67 wt.% PEDOT:PSS, 10 wt.% water, 3.3 wt.% isopropyl alcohol, 11.6 wt.% DMSO, 1.5 wt.% EG and 6.6 wt.% sorbitol. Water was used to dissolve sorbitol. Isopropyl alcohol was used to modify the surface tension and to change the drying process.

The properties of the improved PEDOT:PSS ink with a viscosity 14.1 mPa s and a surface tension of 33.9 mN m^{-2} is similar to the non-improved PEDOT:PSS ink.

The sheet resistance of the improved PEDOT:PSS ink was measured for different layers as is summarized in Tab. 2.

Layers	R_B in Ω/□	α in 1/K
2	19 274.6	−2.7 1E − 3
3	1127.2	−1.9 1E − 3
4	145.5	−1.0 1E − 3

Tab. 2: Properties of the improved printed PEDOT:PSS layers.

R_B of the improved PEDOT:PSS ink (4 layers) could be reduced to 13% of the previous value. Additionally the electrical coefficient of temperature α was measured. As can be seen from Tab. 2 the coefficient is negative and gets lower for thicker layers.

Inkjet Printed Sensor System

As a demonstrator a cantilever with a strain gauge and PEDOT:PSS / NAg thermocouple was printed on a PIOT film (Fig. 5). A resistance for temperature compensation is added. Furthermore 100 Ω lines were printed as series resistances of the SMD LEDs used as further demonstration.

Back-Injection Molding Process

A 3D model (160 mm × 120 mm × 40 mm) of the mold for a cantilever was drawn in PTC Creo Parametric 3.0. The 3D model was printed with an Objet Connex350 3D printer from Stratasys. A photopolymer was used as mold material, which gets cross-linked through exposure to UV light. After cross-linking and removing the necessary support material the mold and was placed in a Victory 50 injection moulding machine from Engel [18]. The PIOT film was fixed in the mold with adhesive tape as shown in Fig. 6.

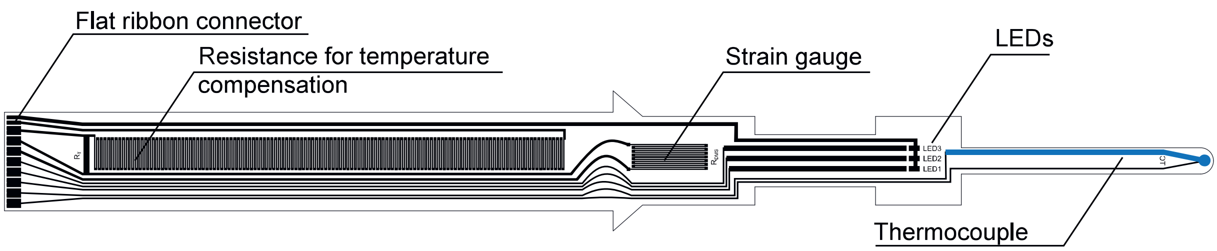

Fig. 5. Layout of the sensor system with a thermocouple, strain gauge and three SMD leds.

DOI 10.5162/sensor2017/D2.3

The clamping force was 200 kN, a higher clamping force destroys the mold and the printed NAg layer. A polyethylene melt was injected with a pressure of 180 bar at a temperature of 200 °C. The temperature is below the melting point of the PIOT film (PET $>$ 250 °C) and above the melting point of polyethylene (115 °C to 135 °C). The released back injected cantilever is shown Fig. 7.

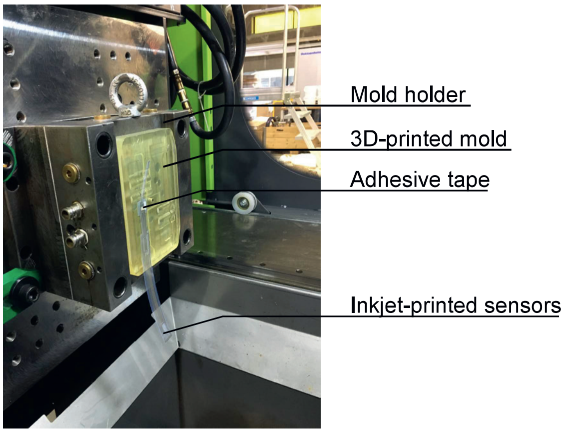

Fig. 6. Fixed PIOT film in an injection molding machine.

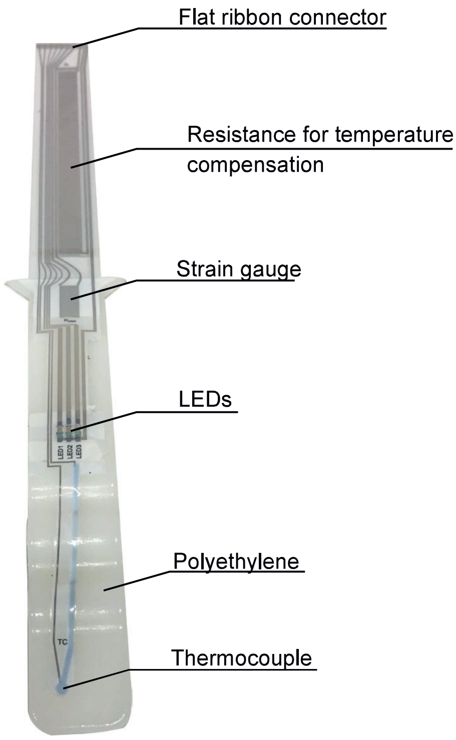

Fig. 7. Back molded PIOT-film with a strain sensor, an NAg-PEDOT:PSS thermocouple and integrated SMD-LEDs.

Results

The temperature-dependent voltage of the thermocouple and resistance change of the strain gauge R_{DMS} were measured with the analog to digital converter (ADC) AD7124-4 as shown in Fig. 8. R_{DMS} and R_T are driven with constant current I_{OUT4}. The voltage over R_T is used as a reference for the ADC, thus compensating for temperature drifts.

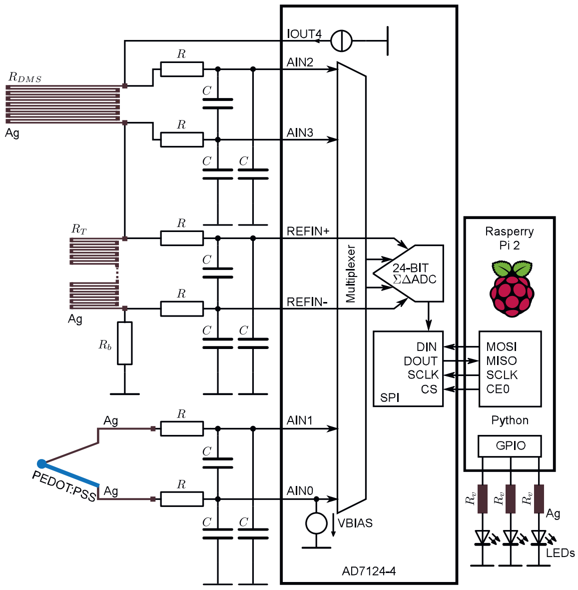

Fig. 8. Block diagram to measure the thermoelectric voltage and strain of the printed sensor system (gray and blue colored).

Conclusion

A sensor system consisting of a strain gauge, a thermocouple and some surface mounted devices (LEDs) were manufactured on a coated PET film. By using the injection molding technology, the inkjet-printed thin film was embedded into polyethylene. The NAg and PEDOT:PSS layers were protected from mechanical and ambient influences. In this context the strain gauge factor of NAg on a PET film and the Seebeck coefficients of different material combinations were characterized.

Acknowledgment

The authors gratefully acknowledge the financial support for the work presented in this paper by Austrian Research Funding Association (FFG) under contact grant 843499 and WimTec Sanitärprodukte GmbH.

References

[1] C. Beisteiner, L. Sonnleithner, and B. Zagar, Erste Experimentelle Untersuchungen von Low-Cost Dehnungsmessstreifen, Tagungsband der 4. Tagung Innovation Messtechnik, 70–75, Shaker Verlag GmbH, Aachen (2015)

[2] S. Duby, B. J. Ramsey, and D. J. Harrison, Printed thick-film thermocouple sensors, *Electronics Letters*, 41 (6); (2005) 312–314

[3] D. Tolfree and M. Jackson, Commercializing Micro-Nanotechnology Products, CRC Press

(2007)

[4] C. Beisteiner, R. Gstöttenmayr, T. Altmanninger, and B. G. Zagar, Electrical and mechanical characterization of inkjet-printed functional structures, Oldenbourg Wissenschaftsverlag GmbH (2016)

[5] S. Hoath, Fundamentals of Inkjet Printing: The Science of Inkjet and Droplets (2016)

[6] R. Leach, The Printing Ink Manual: 4th edition, Springer US (2012)

[7] AND Tuning Fork Vibro Viscometers, http://www.aandd.jp, visited on April 3, 2017

[8] SITA DynoTester, http://www.sita-process.com, visited on April 3, 2017

[9] F. Hejda, P. Solar, and J. Kousal, Surface free energy determination by contact angle measurements–A comparison of various approaches

[10] R. Wallner, Flexible ink-jet printed 2D strain gauge sensor, Master thesis (2016)

[11] J. Kim, Z. Wang, and W. S. Kim, Stretchable RFID for Wireless Strain Sensing With Silver Nano Ink, *IEEE Sensors Journal*, 14 (12); (2014) 4395–4401, doi:10.1109/JSEN.2014.2335743

[12] L. Rebenklau, P. Gierth, A. Paproth, K. Irrgang, L. Lippmann, A. Wodtke, L. Niedermeyer, K. Augsburg, and F. Bechtold, Temperature sensors based on thermoelectric effect, 2015 European Microelectronics Packaging Conference (EMPC), 1–5 (2015)

[13] M. Schagerl, Y. J. Zhao, C. Beisteiner, and S. Gschossmann, An Inkjet-Printed Carbon Nanotubes Strain Distribution Sensor for Quasi Real-Time Strain Monitoring of Lightweight Design Materials, 7th Forum on New Materials - Part E, vol. 101 of *Advances in Science and Technology*, 3–8, Trans Tech Publications (2017)

[14] Clevios Conductive Polymers - Heraeus, http://www.heraeus.com, visited on April 3, 2017

[15] US Research Nanomaterials, Inc., http://www.us-nano.com, visited on April 3, 2017

[16] Q. Wei, M. Mukaida, K. Kirihara, Y. Naitoh, and T. Ishida, Recent Progress on PEDOT-Based Thermoelectric Materials, *Materials*, 8 (2); (2015) 732–750

[17] A. Nardes, M. Kemerink, M. de Kok, E. Vinken, K. Maturova, and R. Janssen, Conductivity, work function, and environmental stability of PEDOT:PSS thin films treated with sorbitol, *Organic Electronics*, 9 (5); (2008) 727 – 734, doi:http://dx.doi.org/10.1016/j.orgel.2008.05.006

[18] T. Mitterlehner, C. Beisteiner, J. Rieger, P. Dunzendorfer, and G. Steinbichler, Back injection molding with additiv manufactured mold inserts using all-inkjet printed substrates, Technical conference of the Society of Plastics Engineers, ANTEC (2017)